Linear OPF-based Robust Dynamic Operating Envelopes with Uncertainties in Unbalanced Distribution Networks

Bin Liu, *Member*, *IEEE*, Julio H. Braslavsky, *Senior Member*, *IEEE*, and Nariman Mahdavi

***Abstract*—Dynamic operating envelopes (DOEs), as a key enabler to facilitate distributed energy resource (DER) integration, have attracted increasing attention in the past years. However, uncertainties, which may come from load forecasting errors or inaccurate network parameters, have been rarely discussed in DOE calculation, leading to compromised quality of the hosting capacity allocation strategy. This letter studies how to calculate DOEs that are immune to such uncertainties based on a linearised unbalanced three-phase optimal power flow (UTOPF) model. With uncertain parameters constrained by norm balls, formulations for calculating robust DOEs (RDOEs) are presented along with discussions on their tractability. Two cases, including a 2-bus illustrative network and a representative Australian network, are tested to demonstrate the effectiveness and efficiency of the proposed approach.**

***Index Terms*—Distributed energy resource (DER), dynamic operating envelope (DOE), feasible region, robust optimisation, uncertainty modelling, unbalanced optimal power flow.**

I. Introduction

THE penetration of distributed energy resources (DERs) has been rapidly increasing worldwide in the past years, leading to a series of issues that require close coordination among transmission system operators (TSOs), distribution system operators (DSOs), and emerging DER aggregators via virtual power plants (VPPs) [1], [2]. Dynamic operating envelope (DOE), which specifies the operational range for customers with DERs at the connection point that is permissible within the network operational limits, is identified as a key enabler in future power system architectures and has gained increasing interest from both industry and academia to manage DER export/import limits and to facilitate DER participation in electricity markets [2]. Differing from static operating envelopes (SOEs) that are calculated based on the worst operational scenarios that occur rarely in a distribution network, DOEs can be updated more frequently (day-ahead, every several hours, hourly, or every 15 min) to avoid unnecessary limitations on DER integration and free up the latent network hosting capacity. Moreover, compared with the co-optimisation of scheduled generators, DERs, and network operations, DOEs can be calculated and published by an individual distribution system operator to avoid traceability issues that may arise when both transmission networks and medium-/low-voltage distribution networks are modelled and optimised together by a single central system operator.

Although substantial advances have been made in developing approaches to calculating DOEs in recent years [1], [3], [4], uncertainties, which may arise from load forecasting and inaccurate network parameters, are typically ignored in the calculations, which may lead to unreliable DOE allocations. To address this issue, this letter proposes an approach to calculate robust DOEs (RDOEs) that are immune to such uncertainties. It is noteworthy that DOEs are inherently linked to the concept of feasible region (FR), which has been discussed for transmission networks in [5] and for distribution networks in [6]. Geometrically, each DOE allocation strategy is linked to a feasible point on the boundary of the FR when it is calculated by deterministic approaches such as in [3] and [4]. The contributions of this letter are summarised as follows.

1) The formulation of the FR for DERs, along with its appropriate reformulation, is presented based on a linearised unbalanced three-phase optimal power flow (UTOPF) model. Formulating the FR first is for the convenience of considering uncertainties from network impedances and/or forecasting errors.

2) The robust feasible region (RFR), which is a variation of the FR, while considering the studied uncertainties modelled as norm inequalities, is presented based on static robust optimisation theory, leading to deterministic convex formulations for calculating RDOEs.

The proposed approach is tested and demonstrated efficiently on a 2-bus illustrative network and a representative Australian network.

Manuscript received: September 10, 2023; revised: October 20, 2023; accepted: November 1, 2023. Date of CrossCheck: November 1, 2023. Date of online publication: November 22, 2023.

This work was supported by the CSIRO Strategic Project on Network Optimisation & Decarbonisation (No. OD-107890).

B. Liu (corresponding author) was with Energy Centre, Commonwealth Scientific and Industrial Research Organisation (CSIRO), Newcastle 2300, Australia, and he is now with the Network Planning Division, Transgrid, Sydney 2000, Australia (e-mail: eeliubin@ieee.org).

J. H. Braslavsky and N. Mahdavi are with the Energy Systems Program, Energy Centre, Commonwealth Scientific and Industrial Research Organisation (CSIRO), Newcastle 2300, Australia (e-mail: julio.braslavsky@csiro.au; nariman.mahdavimazdeh@csiro.au).

DOI: 10.35833/MPCE.2023.000653

II. Calculating DOEs via Deterministic UTOPF

Based on UTOPF, a deterministic approach to calculating DOEs can be formulated as:

$$\max_{P_m, Q_m} r(\boldsymbol{P}) \tag{1}$$

$$V_{i_{\mathrm{ref}}}^{\phi} = V_0^{\phi} \quad \forall \phi \tag{2}$$

$$V_i^{\phi} - V_j^{\phi} = \sum_{\psi} z_{ij}^{\phi\psi} I_{ij}^{\phi} \quad \forall \phi, \forall ij \tag{3}$$

$$\sum_{n:n\to i} I_{ni}^{\phi} - \sum_{m:i\to m} I_{im}^{\phi} = \sum_{m} \frac{\mu_{\phi,i,m}(P_m - \mathrm{j}Q_m)}{(V_i^{\phi})^*} \quad \forall \phi, \forall i \neq i_{\mathrm{ref}} \tag{4}$$

$$V_i^{\min} \leq \left|V_i^{\phi}\right| \leq V_i^{\max} \quad \forall \phi, \forall i \tag{5}$$

where $r(\boldsymbol{P})$ is the objective function reflecting the efficiency and fairness in calculating DOEs, and can be in linear or convex quadratic forms; i_{ref} is the index of the reference bus; V_0^{ϕ} is the fixed voltage of phase ϕ at reference bus (known parameter); $V_i^{\phi} (i \neq 0)$ is the voltage of phase ϕ at node i; I_{ni}^{ϕ} is the current in phase ϕ of line ni flowing from bus n to bus i; $\mu_{\phi,i,m} \in \{0,1\}$ is a parameter indicating the phase connection of customer m with its value being 1 if it is connected to phase ϕ of bus i and being 0 otherwise; $V_i^{\min}$ and $V_i^{\max}$ are the lower and upper limits of $\left|V_i^{\phi}\right|$, respectively; P_m is the active power demand of customer m; and Q_m is the reactive power demand of customer m. For simplicity, all P_m and Q_m are treated as variables in the formulation. However, they will be fixed to their forecasting values if they are uncontrollable.

In the formulation, the objective function aims at maximising $r(\boldsymbol{P})$ to obtain the desired DOEs, subject to (2) specifying the voltage at the reference bus, (3) formulating voltage drop in each line, (4) assuring that Kirchhoff's current law is satisfied, and (5) representing voltage magnitude (VM) constraints. It is noteworthy that only VM constraints are considered in this letter; however, other constraints can be conveniently incorporated.

Note that for most distribution networks, the differences of voltage angles in each phase are sufficiently small [7] and nodal voltages throughout the network are around 1.0 p.u., (4) can be linearised by fixing V_i^{ϕ} in the denominator on the right-hand side of (5), leading to a compact formulation of (1)-(5) with linear constraints as:

$$\max_{\boldsymbol{p}_1, \boldsymbol{q}_1} r(\boldsymbol{p}_1) \tag{6}$$

$$[\boldsymbol{A}_1, \boldsymbol{A}_2][\boldsymbol{p}_1^{\mathrm{T}}, \boldsymbol{p}_2^{\mathrm{T}}]^{\mathrm{T}} + [\boldsymbol{B}_1, \boldsymbol{B}_2][\boldsymbol{q}_1^{\mathrm{T}}, \boldsymbol{q}_2^{\mathrm{T}}]^{\mathrm{T}} + \boldsymbol{C}\boldsymbol{l} = \boldsymbol{b} \tag{7}$$

$$\boldsymbol{D}\boldsymbol{v} + \boldsymbol{E}\boldsymbol{l} = \boldsymbol{d} \tag{8}$$

$$\boldsymbol{F}\boldsymbol{v} \leq \boldsymbol{f} \tag{9}$$

where $\boldsymbol{p}_1$ and $\boldsymbol{p}_2$ are the vectors related to active power from active customers (VPP participants) and passive customers (the customers for which active power needs to be forecasted or estimated), respectively; $\boldsymbol{q}_1$ and $\boldsymbol{q}_2$ are the vectors consisting of reactive power that is controllable and that needs to be forecasted or estimated, respectively; $\boldsymbol{l}$ and $\boldsymbol{v}$ are the vectors consisting of state variables related to line currents and nodal voltages, respectively; and $\boldsymbol{A} = [\boldsymbol{A}_1, \boldsymbol{A}_2]$, $\boldsymbol{B} = [\boldsymbol{B}_1, \boldsymbol{B}_2]$, $\boldsymbol{C}$, $\boldsymbol{b}$, $\boldsymbol{D}$, $\boldsymbol{E}$, $\boldsymbol{d}$, $\boldsymbol{F}$, and $\boldsymbol{f}$ are the constant parameters with appropriate dimensions.

It is noteworthy that the fixed value of V_i^{ϕ}, i.e., $\bar{V}_i^{\phi}$, can be estimated, for example, as $1.0\angle 0°$ p.u., $1.0\angle 120°$ p.u., and $1.0\angle -120°$ p.u. for phases a, b, and c, respectively, or acquired from measurements from the network to improve the accuracy of the linearised formulation further. More details on the linearisation accuracy will be presented and discussed in Section IV.

In the formulation, (7) links back to (4) after linearisation and represents the relations between line currents $\boldsymbol{l}$ and residential demands $\boldsymbol{p}_1$, $\boldsymbol{p}_2$, $\boldsymbol{q}_1$, and $\boldsymbol{q}_2$; (8) represents the linearised power flow equations that link the bus voltages $\boldsymbol{v}$ and currents $\boldsymbol{l}$ running in all lines, i.e., (2) and (3); and (9) represents all the operational constraints after the linearisation, i.e., (5).

Noting that only $\boldsymbol{p}_1$ and $\boldsymbol{q}_1$ are independent variables, (2) defines the FR as a function of $\boldsymbol{q}_1$ for $\boldsymbol{p}_1$. Therefore, if all realised values of $\boldsymbol{p}_1$ fall within the FR, the integrity of the network can be guaranteed. After removing state variables $\boldsymbol{v}$ and $\boldsymbol{l}$, the FR for $\boldsymbol{p}_1$ can be expressed as the following polyhedron.

$$\begin{aligned}\mathcal{F}(\boldsymbol{q}_1) = \{\boldsymbol{p}_1 | \boldsymbol{F}\boldsymbol{D}^{-1}\boldsymbol{E}\boldsymbol{C}^{-1}(\boldsymbol{A}_1\boldsymbol{p}_1 + \boldsymbol{A}_2\boldsymbol{p}_2 + \boldsymbol{B}[\boldsymbol{q}_1^{\mathrm{T}}, \boldsymbol{q}_2^{\mathrm{T}}]^{\mathrm{T}} - \boldsymbol{b}) \leq \\ \boldsymbol{f} - \boldsymbol{F}\boldsymbol{D}^{-1}\boldsymbol{d}\}\end{aligned} \tag{10}$$

It is noteworthy that both $\boldsymbol{C}$ and $\boldsymbol{D}$ can be proven to be invertible since both of them can be constructed from the connectivity matrix of all buses (excluding the reference bus) and all lines in a distribution network with radial topology. Further, for the convenience of later discussions, we have the following proposition and its proof.

Proposition 1: the FR expressed as (10) is equivalent to:

$$\mathcal{F}(\boldsymbol{q}_1) = \{\boldsymbol{p}_1 | vec(\boldsymbol{E})^{\mathrm{T}}\boldsymbol{H}_i(\boldsymbol{A}_1\boldsymbol{p}_1 + \boldsymbol{A}_2\boldsymbol{p}_2 + \boldsymbol{B}[\boldsymbol{q}_1^{\mathrm{T}}, \boldsymbol{q}_2^{\mathrm{T}}]^{\mathrm{T}} - \boldsymbol{b}) \leq \boldsymbol{t}_i, \forall i\} \tag{11}$$

where $vec(\cdot)$ is the vectorising operator for a matrix. For example, for $\boldsymbol{H} = \begin{bmatrix} h_{11} & h_{12} \\ h_{21} & h_{22} \end{bmatrix}$, we have $vec(\boldsymbol{H}) = [h_{11}, h_{21}, h_{12}, h_{22}]^{\mathrm{T}}$. $[\cdot]_i$ indicates the i^{th} row of a matrix or the i^{th} element of a vector. $\boldsymbol{H}_i = \boldsymbol{C}^{-1} \otimes ([\boldsymbol{F}]_i\boldsymbol{D}^{-1})^{\mathrm{T}}$ with $\otimes$ being the Kronecker product, and $\boldsymbol{t}_i = [\boldsymbol{f} - \boldsymbol{F}\boldsymbol{D}^{-1}\boldsymbol{d}]_i$.

Proof: from (10), it is obvious that the i^{th} inequality expression is:

$$[\boldsymbol{F}]_i\boldsymbol{D}^{-1}\boldsymbol{E}\boldsymbol{C}^{-1}(\boldsymbol{A}_1\boldsymbol{p}_1 + \boldsymbol{A}_2\boldsymbol{p}_2 + \boldsymbol{B}[\boldsymbol{q}_1^{\mathrm{T}}, \boldsymbol{q}_2^{\mathrm{T}}]^{\mathrm{T}} - \boldsymbol{b}) \leq [\boldsymbol{f} - \boldsymbol{F}\boldsymbol{D}^{-1}\boldsymbol{d}]_i = \boldsymbol{t}_i \tag{12}$$

For the term $[\boldsymbol{F}]_i\boldsymbol{D}^{-1}\boldsymbol{E}\boldsymbol{C}^{-1}$, we have [8]:

$$vec([\boldsymbol{F}]_i\boldsymbol{D}^{-1}\boldsymbol{E}\boldsymbol{C}^{-1}) = (\boldsymbol{C}^{-\mathrm{T}} \otimes [\boldsymbol{F}]_i\boldsymbol{D}^{-1})vec(\boldsymbol{E}) \tag{13}$$

Equation (13) leads to:

$$vec(\boldsymbol{E})^{\mathrm{T}}(\boldsymbol{C}^{-1} \otimes ([\boldsymbol{F}]_i\boldsymbol{D}^{-1})^{\mathrm{T}})\boldsymbol{w} = [\boldsymbol{F}]_i\boldsymbol{D}^{-1}\boldsymbol{E}\boldsymbol{C}^{-1}\boldsymbol{w} \tag{14}$$

where $\boldsymbol{w} = \boldsymbol{A}_1\boldsymbol{p}_1 + \boldsymbol{A}_2\boldsymbol{p}_2 + \boldsymbol{B}[\boldsymbol{q}_1^{\mathrm{T}}, \boldsymbol{q}_2^{\mathrm{T}}]^{\mathrm{T}} - \boldsymbol{b}$, which proves the proposition.

Therefore, seeking DOEs through the deterministic approach with controllable $\boldsymbol{q}_1$ is equivalent to solving:

$$\max_{(\boldsymbol{p}_1, \boldsymbol{q}_1)} \{r(\boldsymbol{p}_1) | \text{s.t. } \boldsymbol{p}_1 \in \mathcal{F}(\boldsymbol{q}_1)\} \tag{15}$$

And one typical formulation of the objective function, which will be used in this letter, is $r(\boldsymbol{p}_1) = \boldsymbol{1}^{\mathrm{T}}\boldsymbol{p}_1$.

III. ROBUST DOEs

A. Uncertainty Modelling

Comparing (1) and (2), the errors in forecasting P_m and Q_m, and the inaccuracies in $z_{ij}^{\phi\psi}$ will lead to uncertainties in $\boldsymbol{p}_2$, $\boldsymbol{q}_2$, and $\boldsymbol{E}$, respectively. In this letter, such uncertainties are formulated as:

$$\begin{aligned}\mathcal{E}=\mathcal{E}_1\cap\mathcal{E}_2=&\{\boldsymbol{E}|vec(\boldsymbol{E})=\boldsymbol{e}_1+\boldsymbol{J}_1\boldsymbol{x},\|\boldsymbol{x}\|_\infty\le\gamma_1\}\cap\\&\{\boldsymbol{E}|vec(\boldsymbol{E})=\boldsymbol{e}_2+\boldsymbol{J}_2\boldsymbol{x},\|\boldsymbol{x}\|\le\gamma_2\}\end{aligned}\tag{16}$$

$$\begin{aligned}\mathcal{P}=\mathcal{P}_1\cap\mathcal{P}_2=&\{\boldsymbol{p}_2|\boldsymbol{p}_2=\boldsymbol{u}_1+\boldsymbol{U}_1\boldsymbol{y},\|\boldsymbol{y}\|_\infty\le\rho_1\}\cap\\&\{\boldsymbol{p}_2|\boldsymbol{p}_2=\boldsymbol{u}_2+\boldsymbol{U}_2\boldsymbol{y},\|\boldsymbol{y}\|\le\rho_2\}\end{aligned}\tag{17}$$

$$\begin{aligned}\mathcal{Q}=\mathcal{Q}_1\cap\mathcal{Q}_2=&\{\boldsymbol{q}_2|\boldsymbol{q}_2=\boldsymbol{w}_1+\boldsymbol{W}_1\boldsymbol{z},\|\boldsymbol{z}\|_\infty\le\theta_1\}\cap\\&\{\boldsymbol{q}_2|\boldsymbol{q}_2=\boldsymbol{w}_2+\boldsymbol{W}_2\boldsymbol{z},\|\boldsymbol{z}\|\le\theta_2\}\end{aligned}\tag{18}$$

where $\boldsymbol{e}_i$, $\boldsymbol{u}_i$, $\boldsymbol{w}_i$, $\boldsymbol{J}_i$, $\boldsymbol{U}_i$, $\boldsymbol{W}_i$, γ_i, ρ_i, and θ_i are the constant parameters describing the uncertainty sets; and $\boldsymbol{x}$, $\boldsymbol{y}$, and $\boldsymbol{z}$ are the random variables; and the ∞-norm constraint in $\mathcal{E}_1$, $\mathcal{P}_1$, and $\mathcal{Q}_1$ provides a general lower/upper bound for the random variable, while the norm constraint in $\mathcal{E}_2$, $\mathcal{P}_2$, and $\mathcal{Q}_2$, which can take 1-/2-/∞-norm or other types of norms, is to further reduce the conservativeness of the uncertainty set.

Several remarks on uncertainty modelling are given below.

1) Constant parameters can be chosen depending on the physical truth or historical error distributions. For example, if $\boldsymbol{E}$ is usually within 10% error of $\bar{\boldsymbol{E}}$, where $\bar{\boldsymbol{E}}$ is the nominal value of $\boldsymbol{E}$, we can set $\mathcal{E}=\mathcal{E}_1$, $\boldsymbol{e}_1=vec(\bar{\boldsymbol{E}})$, $\boldsymbol{J}_1=diag(\boldsymbol{e}_1)$, and γ_1. As another example, if $\boldsymbol{p}_2$ falls in $[0,p_2^{\max}]$ and its forecasting error follows a multivariate normal distribution with expectation and covariance being 0 and $\boldsymbol{\Sigma}$, respectively, and 2-norm is used in $\mathcal{P}_2$, $\boldsymbol{u}_1$ can be set as a vector with all its elements being $p_2^{\max}/2$, $\boldsymbol{U}_1=diag(\boldsymbol{u}_1)$, and $\rho_1=1$ for $\mathcal{P}_1$. Note that $\boldsymbol{y}^{\mathrm{T}}\boldsymbol{\Sigma}\boldsymbol{y}$ follows a Chi-square distribution with freedom degrees of n, i.e., $\boldsymbol{y}^{\mathrm{T}}\boldsymbol{\Sigma}\boldsymbol{y}\sim\chi_n^2$, we can set $\boldsymbol{u}_2=\bar{\boldsymbol{p}}_2$ in $\mathcal{P}_2$, with $\bar{\boldsymbol{p}}_2$ being the forecasted value of $\boldsymbol{p}_2$. $\boldsymbol{U}_2=diag(\boldsymbol{u}_2)$ and $\rho_2=(\chi_{n,1-\epsilon}^2)^{1/2}$ so as to guarantee that $\boldsymbol{p}_2$ now falls within $\mathcal{P}_2$ with a confidence level of $1-\epsilon$.

2) Constant parameters can also be chosen depending on the confidence level of satisfying (11), leading to equivalent chance-constrained optimisation problems. This, however, is beyond the scope of this letter, and more discussions can be found in [9].

3) $\mathcal{E}$, $\mathcal{P}$, and $\mathcal{Q}$ can be formulated as other types of convex sets, which, however, may affect the tractability of the formulated problem if two or more uncertainties co-exist. More discussions will be provided in the next section.

B. Robust DOEs

For the convenience of discussion, we here assume that both $\boldsymbol{q}_1$ and $\boldsymbol{q}_2$ are controllable, thus removing uncertainties in $\boldsymbol{q}_2$. However, similar to dealing with uncertainty in $\boldsymbol{p}_2$, the proposed approach can be easily extended to the case when uncertainty in $\boldsymbol{q}_2$ exists.

Since the optimisation problem (15) only contains linear inequality constraints (11), the essential idea in seeking RDOEs is to make sure that (11) is always satisfied for any realisation of uncertain parameters. To obtain the robust counterpart (RC) of (15), the equivalent reformulation of (11), considering the uncertainties that are bounded by (16)-(18), should be derived. Taking a generic formulation $f(\varepsilon,x)\le 0$ as an example, where x is a variable and ε is an uncertain parameter belonging to $\mathcal{E}=\{g(\varepsilon)\le 0\}$, its RC formulation is:

$$\max_{\varepsilon\in\mathcal{E}} f(\varepsilon,x)=\min_{\alpha\ge 0}\max_{\varepsilon} f(\varepsilon,x)-\alpha g(\varepsilon)\le 0\tag{19}$$

With the following fact or assumption, (19) can then be reformulated as deterministic linear or other convex constraints.

1) If the min operator is on the left-hand side of a less-than-or-equal-to constraint, it can be safely removed. For example, $h(x,\beta)\le 0$ can always guarantee that $\min_{\beta} h(x,\beta)\le 0$.

2) Under certain circumstances, for example, $f(\varepsilon,x)$ being linear and $\mathcal{E}$ being norm constraints, i.e., $\mathcal{E}=\{\varepsilon|\varepsilon\le\bar{\varepsilon}\}$, $\max_{\varepsilon} f(\varepsilon,x)-\alpha g(\varepsilon)$ can be expressed in an equivalent deterministic form without the max operator.

Next, we will discuss how such reformulation techniques can be applied in deriving the RDOE formulation under various uncertainty models.

1) With Uncertainty Only in $\boldsymbol{E}$

Fixing $\boldsymbol{p}_2$ at $\bar{\boldsymbol{p}}_2$ and denoting $\boldsymbol{h}_i=\boldsymbol{H}_i(\boldsymbol{A}_1\boldsymbol{p}_1+\boldsymbol{A}_2\bar{\boldsymbol{p}}_2+\boldsymbol{B}\boldsymbol{q}-\boldsymbol{b})$, the inequality expression in (11) with any realisation of uncertain $\boldsymbol{E}$ is equivalent to:

$$\max_{\boldsymbol{E}\in\mathcal{E}} vec(\boldsymbol{E})^{\mathrm{T}}\boldsymbol{H}_i(\boldsymbol{A}_1\boldsymbol{p}_1+\boldsymbol{A}_2\bar{\boldsymbol{p}}_2+\boldsymbol{B}\boldsymbol{q}-\boldsymbol{b})=\delta^*(\boldsymbol{h}_i|\mathcal{E})\le\boldsymbol{t}_i\tag{20}$$

For the left-hand side of (20), we further have:

$$\begin{aligned}&\max_{\boldsymbol{E}\in\mathcal{E}} vec(\boldsymbol{E})^{\mathrm{T}}\boldsymbol{H}_i(\boldsymbol{A}_1\boldsymbol{p}_1+\boldsymbol{A}_2\bar{\boldsymbol{p}}_2+\boldsymbol{B}\boldsymbol{q}-\boldsymbol{b})=\delta^*(\boldsymbol{h}_i|\mathcal{E})=\\&\min_{\boldsymbol{\tau}_{i1},\boldsymbol{\tau}_{i2}}\{\delta^*(\boldsymbol{\tau}_{i1}|\mathcal{E}_1)+\delta^*(\boldsymbol{\tau}_{i2}|\mathcal{E}_2)|\boldsymbol{\tau}_{i1}+\boldsymbol{\tau}_{i2}=\boldsymbol{h}_i\}=\\&\min_{\boldsymbol{\tau}_{i1},\boldsymbol{\tau}_{i2}}\left\{\sum_j(\boldsymbol{e}_j^{\mathrm{T}}\boldsymbol{\tau}_{ij}+\delta^*(\boldsymbol{J}_j^{\mathrm{T}}\boldsymbol{\tau}_{ij}|\mathcal{X}_j))\middle|\sum_j\boldsymbol{\tau}_{ij}=\boldsymbol{h}_i\right\}\end{aligned}\tag{21}$$

where $\boldsymbol{e}_j$ and $\boldsymbol{J}_j$ are the same as those defined in (16); and $\boldsymbol{\tau}_{ij}$ is an intermediate variable.

We can then obtain:

$$\min_{\boldsymbol{\tau}_{i1},\boldsymbol{\tau}_{i2}}\left\{\sum_j\boldsymbol{e}_j^{\mathrm{T}}\boldsymbol{\tau}_{ij}+\gamma_1\left\|\boldsymbol{J}_1^{\mathrm{T}}\boldsymbol{\tau}_{i1}\right\|_1+\gamma_2\left\|\boldsymbol{J}_2^{\mathrm{T}}\boldsymbol{\tau}_{i2}\right\|_*\middle|\sum_j\boldsymbol{\tau}_{ij}=\boldsymbol{h}_i\right\}\tag{22}$$

where $\delta^*(\boldsymbol{y}|\mathcal{X})=\sup_{\boldsymbol{x}\in\mathcal{X}}\boldsymbol{y}^{\mathrm{T}}\boldsymbol{x}$ is the conjugate function of the support function $\delta(\boldsymbol{x}|\mathcal{X})$; $\mathcal{X}_1=\left\{\boldsymbol{x}\middle|\|\boldsymbol{x}\|_\infty\le\gamma_1\right\}$; $\mathcal{X}_2=\left\{\boldsymbol{x}\middle|\|\boldsymbol{x}\|\le\gamma_2\right\}$; and $\|\cdot\|_*$ represents the dual norm operator. Moreover, $\delta^*(\boldsymbol{y}|\mathcal{X})$ is always a convex function [10].

After safely removing the min operator in (22), (20) can be reformulated as [9]:

$$\sum_j\boldsymbol{e}_j^{\mathrm{T}}\boldsymbol{\tau}_{ij}+\gamma_1\left\|\boldsymbol{J}_1^{\mathrm{T}}\boldsymbol{\tau}_{i1}\right\|_1+\gamma_2\left\|\boldsymbol{J}_2^{\mathrm{T}}\boldsymbol{\tau}_{i2}\right\|_*\le\boldsymbol{t}_i\tag{23}$$

$$\sum_j\boldsymbol{\tau}_{ij}=\boldsymbol{h}_i\tag{24}$$

As a result, (23) and (24) define the robust FR (RFR) that is robust to uncertain $\boldsymbol{E}$, and maximising $r(\boldsymbol{p}_1)$ over $(\boldsymbol{p}_1,\boldsymbol{q},\boldsymbol{\tau}_{ij})$ in this RFR will report the desired RDOEs. The final optimisation problem with the objective maximising the total DOE can be formulated as $\max_{\boldsymbol{p}_1,\boldsymbol{q}}\{r(\boldsymbol{p}_1)|\text{s.t. (23), (24)}\}$.

2) With Uncertainty Only in $\boldsymbol{p}_2$

With $vec(\boldsymbol{E})$ fixed at $\bar{\boldsymbol{e}}$ and denoting $\boldsymbol{g}_i = \boldsymbol{A}_2^{\mathrm{T}} \boldsymbol{H}_i^{\mathrm{T}} \bar{\boldsymbol{e}}$, for the i^{th} constraint in (11), reformulating (11) while considering uncertainty in $\boldsymbol{p}_2$ leads to:

$$\max_{\boldsymbol{p}_2 \in} \boldsymbol{g}_i^{\mathrm{T}} \boldsymbol{p}_2 = \delta^*(\boldsymbol{g}_i|\mathcal{P}) = \min_{\boldsymbol{\phi}_{i1},\boldsymbol{\phi}_{i2}} \{\delta^*(\boldsymbol{\phi}_{i1}|\mathcal{P}_1) + \delta^*(\boldsymbol{\phi}_{i2}|\mathcal{P}_2)) | \boldsymbol{\phi}_{i1} + \boldsymbol{\phi}_{i2} = \boldsymbol{g}_i\} = \min_{\boldsymbol{\phi}_{i1},\boldsymbol{\phi}_{i2}} \left\{ \sum_j (\boldsymbol{u}_j^{\mathrm{T}} \boldsymbol{\phi}_{ij} + \delta^*(\boldsymbol{U}_j^{\mathrm{T}} \boldsymbol{\phi}_{ij} | \mathcal{Y}_j)) \middle| \sum_j \boldsymbol{\phi}_{ij} = \boldsymbol{g}_i \right\} \tag{25}$$

where $\boldsymbol{\phi}_{ij}$ is an intermediate variable.

We can then obtain:

$$\min_{\boldsymbol{\phi}_{i1},\boldsymbol{\phi}_{i2}} \left\{ \sum_j \boldsymbol{u}_j^{\mathrm{T}} \boldsymbol{\phi}_{ij} + \rho_1 \left\| \boldsymbol{U}_1^{\mathrm{T}} \boldsymbol{\phi}_{i1} \right\|_1 + \rho_2 \left\| \boldsymbol{U}_2^{\mathrm{T}} \boldsymbol{\phi}_{i2} \right\|_* \middle| \sum_j \boldsymbol{\phi}_{ij} = \boldsymbol{g}_i \right\} \le \boldsymbol{t}_i - \bar{\boldsymbol{e}}^{\mathrm{T}} \boldsymbol{H}_i (\boldsymbol{A}_1 \boldsymbol{p}_1 + \boldsymbol{B}\boldsymbol{q} - \boldsymbol{b}) \tag{26}$$

where $\mathcal{Y}_1 = \left\{ \boldsymbol{y} \middle| \left\| \boldsymbol{y} \right\|_\infty \le \rho_1 \right\}$; and $\mathcal{Y}_2 = \left\{ \boldsymbol{y} \middle| \left\| \boldsymbol{y} \right\| \le \rho_2 \right\}$.

Similar to the derivation of the RFR with uncertain $\boldsymbol{E}$, removing the min operator in (26) also leads to an RFR that is robust against uncertain $\boldsymbol{p}_2$. The final optimisation problem to maximise the total DOE can thus be formulated as:

$$\max_{\boldsymbol{p}_1,\boldsymbol{q}} r(\boldsymbol{p}_1) \tag{27}$$

$$\boldsymbol{u}_1^{\mathrm{T}} \boldsymbol{\phi}_{i1} + \boldsymbol{u}_2^{\mathrm{T}} \boldsymbol{\phi}_{i2} + \rho_1 \left\| \boldsymbol{U}_1^{\mathrm{T}} \boldsymbol{\phi}_{i1} \right\|_1 + \rho_2 \left\| \boldsymbol{U}_2^{\mathrm{T}} \boldsymbol{\phi}_{i2} \right\|_* \le \boldsymbol{t}_i - \bar{\boldsymbol{e}}^{\mathrm{T}} \boldsymbol{H}_i (\boldsymbol{A}_1 \boldsymbol{p}_1 + \boldsymbol{B}\boldsymbol{q} - \boldsymbol{b}) \forall i \tag{28}$$

$$\boldsymbol{\phi}_{i1} + \boldsymbol{\phi}_{i2} = \boldsymbol{g}_i \quad \forall i \tag{29}$$

3) With Uncertainties in Both $\boldsymbol{E}$ and $\boldsymbol{p}_2$

In this case, bilinear uncertainty exists in (11), making the RC reformulation generally intractable. However, as discussed in [9], a tractable reformulation is achievable when the uncertainty set follows specific types. One case is when $\mathcal{P}$ is formulated as:

$$\mathcal{P} = \mathcal{P}_1 \cap \mathcal{P}_2 = \left\{ \boldsymbol{p}_2 | \boldsymbol{u} + \boldsymbol{U}\boldsymbol{y}, \boldsymbol{y} \in \mathcal{Y} = \mathcal{Y}_1 \cap \mathcal{Y}_2 \right\} \tag{30}$$

where $\boldsymbol{u} = \boldsymbol{u}_1 = \boldsymbol{u}_2$; $\boldsymbol{U} = \boldsymbol{U}_1 = \boldsymbol{U}_2$; $\mathcal{Y}_1 = \left\{ \boldsymbol{y} \middle| \left\| \boldsymbol{y} \right\|_\infty \le \rho_1 \right\}$; and $\mathcal{Y}_2 = \left\{ \boldsymbol{y} \middle| \left\| \boldsymbol{y} \right\|_1 \le n_t \rho_1 \right\}$ with $n_t \le n$, and n is the cardinality of $\boldsymbol{y}$.

Obviously, there is a total number of $2^{n_t}\binom{n}{n_t}$ extreme points in $\mathcal{Y}$. As a special case, when $n_t = 1$, the $2n$ extreme points in $\mathcal{Y}$ can be expressed as $\{\pm \boldsymbol{y}_1, \ldots, \pm \boldsymbol{y}_k, \ldots, \pm \boldsymbol{y}_n\}$, where $\boldsymbol{y}_k \in \mathbb{R}^{n \times 1}$ is a vector with the k^{th} element being ρ_1 and all the other elements being 0. Based on (22), reformulating the i^{th} constraint in (11) while considering uncertainty in both $\boldsymbol{E}$ and $\boldsymbol{p}_2$ leads to:

$$\min_{\boldsymbol{\tau}_{i1,k},\boldsymbol{\tau}_{i2,k}} \left\{ \sum_j \boldsymbol{e}_j^{\mathrm{T}} \boldsymbol{\tau}_{ij,k} + \gamma_1 \left\| \boldsymbol{J}_1^{\mathrm{T}} \boldsymbol{\tau}_{i1,k} \right\|_1 + \gamma_2 \left\| \boldsymbol{J}_2^{\mathrm{T}} \boldsymbol{\tau}_{i2,k} \right\|_* \middle| \sum_j \boldsymbol{\tau}_{ij,k} = \boldsymbol{h}_i(\boldsymbol{y}_k) \right\} \le \boldsymbol{t}_i \quad \forall k \tag{31}$$

$$\min_{\boldsymbol{\lambda}_{i1,k},\boldsymbol{\lambda}_{i2,k}} \left\{ \sum_j \boldsymbol{e}_j^{\mathrm{T}} \boldsymbol{\lambda}_{ij,k} + \gamma_1 \left\| \boldsymbol{J}_1^{\mathrm{T}} \boldsymbol{\lambda}_{i1,k} \right\|_1 + \gamma_2 \left\| \boldsymbol{J}_2^{\mathrm{T}} \boldsymbol{\lambda}_{i2,k} \right\|_* \middle| \sum_j \boldsymbol{\lambda}_{ij,k} = \boldsymbol{h}_i(-\boldsymbol{y}_k) \right\} \le \boldsymbol{t}_i \quad \forall k \tag{32}$$

where $\boldsymbol{h}_i(\pm \boldsymbol{y}_k) = \boldsymbol{H}_i(\boldsymbol{A}_1 \boldsymbol{p}_1 + \boldsymbol{A}_2 \boldsymbol{u} \pm \boldsymbol{A}_2 \boldsymbol{U} \boldsymbol{y}_k + \boldsymbol{B}\boldsymbol{q} - \boldsymbol{b})$.

Similarly, the final equivalent deterministic formulation to maximise the total DOE can be formulated as:

$$\max_{\boldsymbol{p}_1,\boldsymbol{q}} r(\boldsymbol{p}_1) \tag{33}$$

$$\sum_j \boldsymbol{e}_j^{\mathrm{T}} \boldsymbol{\tau}_{ij,k} + \gamma_1 \left\| \boldsymbol{J}_1^{\mathrm{T}} \boldsymbol{\tau}_{i1,k} \right\|_1 + \gamma_2 \left\| \boldsymbol{J}_2^{\mathrm{T}} \boldsymbol{\tau}_{i2,k} \right\|_* \le \boldsymbol{t}_i \quad \forall i, \forall k \tag{34}$$

$$\sum_j \boldsymbol{e}_j^{\mathrm{T}} \boldsymbol{\lambda}_{ij,k} + \gamma_1 \left\| \boldsymbol{J}_1^{\mathrm{T}} \boldsymbol{\lambda}_{i1,k} \right\|_1 + \gamma_2 \left\| \boldsymbol{J}_2^{\mathrm{T}} \boldsymbol{\lambda}_{i2,k} \right\|_* \le \boldsymbol{t}_i \quad \forall i, \forall k \tag{35}$$

$$\sum_j \boldsymbol{\tau}_{ij,k} = \boldsymbol{h}_i(\boldsymbol{y}_k) \quad \forall i, \forall k \in \{1, 2, \ldots, n\} \tag{36}$$

$$\sum_j \boldsymbol{\lambda}_{ij,k} = \boldsymbol{h}_i(-\boldsymbol{y}_k) \quad \forall i, \forall k \in \{1, 2, \ldots, n\} \tag{37}$$

Several remarks on calculating RDOEs are given below.

1) In this letter, a strictly equal allocation strategy, i. e., DOEs of all active customers being equal to each other, will be used, leading to a linear formulation of the objective function: $r(\boldsymbol{p}_1) = \mathbf{1}^{\mathrm{T}} \boldsymbol{p}_1$ subject to $\boldsymbol{p}_{1,i} = \boldsymbol{p}_{1,j}$ $(\forall i \ne j)$. However, other objective functions can also be applied.

2) Note that (11) is linear in $\boldsymbol{E}$, $\boldsymbol{p}_2$, and $\boldsymbol{q}_2$, a tractable RC for this constraint can always be derived with single uncertainty, i.e., when uncertainty appears only in $\boldsymbol{E}$ or only in $\boldsymbol{p}_2$, and if the uncertainty set is convex. When bilinear uncertainty exists, a tractable RC formulation is achievable if there is a finite number of extreme points for at least one uncertainty set, as shown in (31). However, it can be difficult to enumerate all extreme points itself.

3) The problem (15) with single uncertainty becomes a linear programming (LP) problem when 1-norm or ∞-norm is used in (16)-(18), and becomes second-order cone programming (SOCP) problem when 2-norm is used. However, the RC of (15) with single uncertainty is always a convex programming problem if the uncertainty set is convex.

4) Compared with (11), a buffer term is added to the left side of (11) in its RC, leading to enhanced robustness of the solution. When γ_i, ρ_i, or θ_i equals 0, the RC deteriorates to the deterministic formulation.

5) Due to the unbalances and mutual couplings of all phases in a distribution network and the fact that the active power of a VPP customer may vary between 0 kW and its allocated DOE, there is another type of uncertainty related to the difference between the optimal solution of $\boldsymbol{p}_2$ and its realised value $\hat{\boldsymbol{p}}_2$. Although this is beyond the scope of this letter, such uncertainty can be addressed by: ① taking the approach proposed in [11] on top of an RFR based on the approach proposed in this letter; ② employing the strictly equal allocation strategy, which is already taken in this letter. Note that such an allocation strategy, even with a deterministic DOE calculation approach, can provide satisfactory robustness as demonstrated in [11].

6) When extra constraints on $\boldsymbol{p}_1$ and $\boldsymbol{q}_1$ exist, an additional constraint $\boldsymbol{L}_1 \boldsymbol{p}_1 + \boldsymbol{L}_2 \boldsymbol{p}_2 \le \boldsymbol{r}$ can be added to (10) and (11).

IV. Case Study

A. Case Setup

Two distribution networks, i. e., 2-bus illustrative network and a representative Australian network, will be studied. For the illustrative network, where its topology is presented in Fig. 1, an ideal balanced voltage source with the VM being 1.0 p.u. is connected to bus 1. A three-phase line connects bus 1 and bus 2, and its impedance matrix can be found in [11].

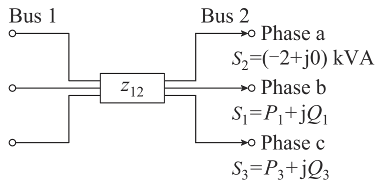

Fig. 1. Network topology of 2-bus illustrative network.

Of the three customers, $S_2 = P_2 + jQ_2$ is fixed, while P_1, P_3, Q_1, and Q_3 are to be optimised with $r(\boldsymbol{P}) = -P_1 - P_3$ and $P_1 = P_3$, aiming at maximising the total exports from customers 1 and 3. Moreover, the default export/import limits for both customers are set to be 7 kW, and controllable reactive power is assumed to be within [−1, 1]kvar. Lower and upper VM limits are set to be 0.95 p.u. and 1.05 p.u., respectively. The representative Australian network has 33 buses and 87 customers, of which 30 are VPP participants whose DOEs are to be calculated. For the remaining 57 customers, their reactive power is fixed, while the active power is treated as uncertain parameters. The default limits on active and reactive power are the same as those in the illustrative network, and other data can be found in [11].

For network impedances, $\boldsymbol{x}$ in (16) refers to the mutual impedances of line 12 for the illustrative network and refers to the positive, negative and zero-sequence impedances of all line codes of lines "46-47", "69-67", "49-50", "40-41", "54-59", "45-50", "67-68", "44-45", "61-62", and "52-54" for the Australian network.

B. Errors from Linearised Model

This subsection will investigate the accuracy of the employed linearised model based on the Australian network, where the given voltages for phases a, b, and c are set to be $1.0\angle 0°$, $1.0\angle -120°$, and $1.0\angle 120°$, respectively, for all buses.

The average and maximum VM errors when the demand for each of the active customers is at 1 kW (low customer load) and 3 kW (high customer load), under both exporting and importing statuses, are presented in Table I. The value 3 kW is taken noting that RDOE calculated for each of the customers is around 3 kW. When customers' demands are at a high level, the average and maximum errors are at around 0.23% and 0.59%, respectively, when they are exporting power to the grid, and are at around 0.83% and 1.78%, respectively, when they are importing power, demonstrating that the linearisation approach can achieve acceptable accuracy for RDOE calculation. However, it is expected that errors will become more significant when true nodal voltages deviate from the given voltage points, which can occur when customers are exporting or importing power at very high levels.

TABLE I
AVERAGE AND THE MAXIMUM VM ERRORS

Customer status	Customer load	VM error (p.u.)	
		Average	The maximum
Export	High	0.002336	0.005877
	Low	0.000125	0.000298
Import	High	0.008268	0.017820
	Low	0.001776	0.003675

The nodal VMs for all three phases of the Australian network are also presented in Fig. 2 when all active customers are exporting at 3 kW, which clearly shows that the VMs calculated by the linearised unbalanced three-phase power flow (LIN-UTPF) and by the non-convex UTPF (NCVX-UTPF) are very close to each other in this scenario.

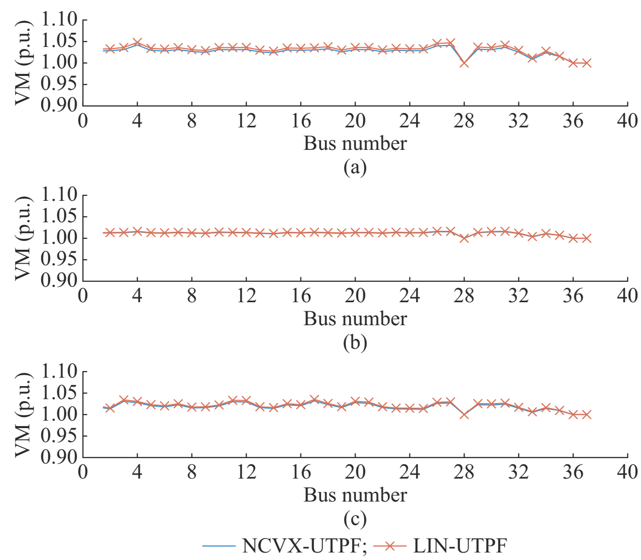

Fig. 2. Nodal VMs for all three phases of Australian network.

However, we admit that the errors brought by the linearisation approach are inevitable, and in some cases, may be high. Thus, more efforts are needed in this area. One of the approaches to improving the accuracy is by iteratively updating the given voltage points used to linearise the model. Specifically, after solving the optimisation model with the optimal solutions of $\boldsymbol{p}$ and $\boldsymbol{q}$ as $\boldsymbol{p}^*$ and $\boldsymbol{q}^*$, respectively, the optimal solution for $\boldsymbol{v}$ after this iteration can be expressed as (38) based on (7) and (8).

$$\boldsymbol{v}^* = \boldsymbol{D}^{-1}\boldsymbol{E}\boldsymbol{C}^{-1}(\boldsymbol{A}\boldsymbol{p}^* + \boldsymbol{B}\boldsymbol{q}^* - \boldsymbol{b}) + \boldsymbol{D}^{-1}\boldsymbol{d} \tag{38}$$

Then, matrix $\boldsymbol{C}$, which depends on the given voltage points, can be updated further, followed by the re-calculation of the RDOE. The effectiveness of the iteration-based approach has been demonstrated in [12] and is omitted here for simplicity.

C. Calculated RDOEs

Simulation results are presented in Table II and Fig. 3 with all optimisation problems solved by Mosek (version 10.0) [13] on a laptop with Intel Core i7-8550U CPU and 16 GB RAM.

TABLE II
DDOEs AND RDOEs AND THEIR COMPUTATIONAL TIME UNDER VARIOUS UNCERTAINTIES

Uncertainty	Norm	Optimal objective (kW)		Computational time (10^{-2} s)	
		2-bus illustrative network	Representative Australian network	2-bus illustrative network	Representative Australian network
Deterministic	Not applicable	–9.9/–13.7	–78.7/–112.3	0.7/0.8	3.7/4.9
$\boldsymbol{E}$	∞-norm (γ_1)	–9.2/–12.8	–49.2/–58.3	4.3/5.4	36.0/57.8
	∞-norm (γ_1)	–8.6/–11.9	–36.3/–43.1	3.9/5.3	36.2/61.6
$\boldsymbol{p}_2$	1-norm (ρ_2)	–9.4/–13.2	–78.1/–111.7	1.0/1.1	44.2/58.3
	2-norm (ρ_2)	–9.4/–13.2	–77.8/–111.4	1.1/0.8	20.2/36.1
	∞-norm (ρ_2)	–9.4/–13.2	–75.4/–109.0	0.7/1.0	68.9/162.6
$(\boldsymbol{E}, \boldsymbol{p}_2)$	(∞, 1)-norm (γ_1, ρ_2)	–8.7/–12.3	–48.7/–56.1	30.0/31.1	2856.0/5839.0

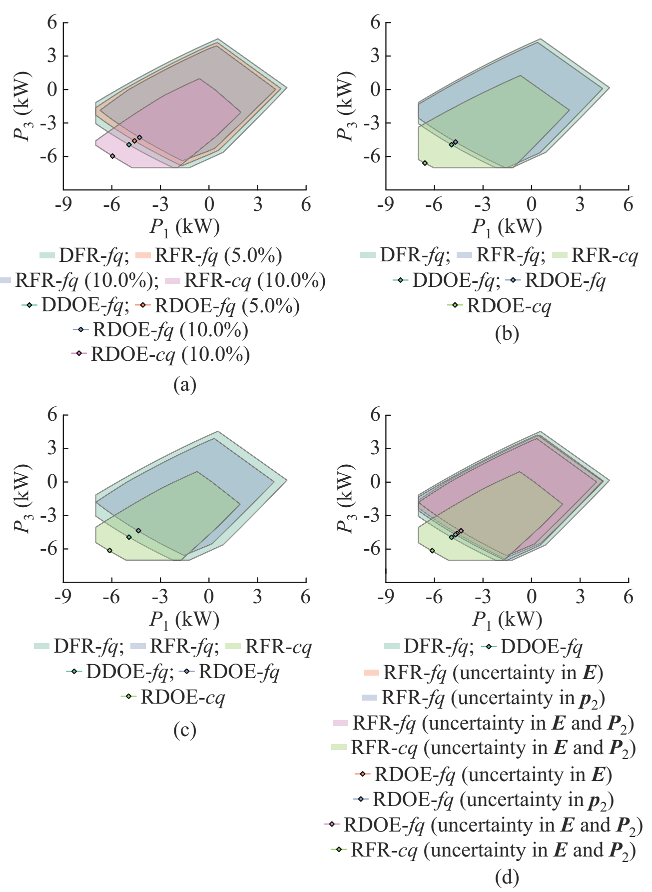

Fig. 3. FRs and DOEs for illustrative network under various uncertainties. (a) Uncertainty in $\boldsymbol{E}$. (b) Uncertainty in $\boldsymbol{p}_2$. (c) Uncertainty in both $\boldsymbol{E}$ and $\boldsymbol{p}_2$. (d) Under various uncertainties.

In Table II, the various uncertainties include: ① $\boldsymbol{q}_1 = \boldsymbol{0}$, $\mathcal{E} = \mathcal{E}_1$ ($\mathcal{E}_2$ is not considered) with $\boldsymbol{e}_1 = vec(\bar{\boldsymbol{E}})$ and $\boldsymbol{J}_1 = diag(\boldsymbol{e}_1)$, and ② $\boldsymbol{p} = \boldsymbol{p}_2$ ($\boldsymbol{p}_1$ is not considered) with $\boldsymbol{u}_2 = \bar{\boldsymbol{p}}_2$ and $\boldsymbol{U}_2 = diag(\boldsymbol{u}_2)$. It should be noted that negative values represent export limits, and numbers on the left-hand and right-hand sides in the table mean with $\boldsymbol{q}_1$ being 0 kvar and with optimised $\boldsymbol{q}_1$, respectively, and the computational time includes both the time for setting up the optimisation model and for solving the optimisaiton problem. In Fig. 3, the legends "DFR" and "RFR" represent the FRs calculated via deterministic and robust approaches, respectively. "DDOE" and "RDOE" indicate the deterministic and robust DOEs, respectively. *fq* means the case when $\boldsymbol{q}_1$ is fixed at 0 kvar while *cq* means $\boldsymbol{q}_1$ is taken as its optimised value.

Moreover, the DOEs calculated by deterministic approach are also presented for comparison purposes. Moreover, the compact formulation of the problems in this paper is realised with the assistance of Julia packages MathOptInterface. jl, JuMP.jl, and PowerModelsDistribution.jl [14].

Simulation results clearly show that RDOEs are more conservative than DDOEs, and a higher level of uncertainty leads to a more conservative allocation strategy, as demonstrated in Fig. 3(a). Moreover, as shown in Table II and Fig. 3, RFRs and allocated DOEs with optimised controllable reactive power can effectively report ameliorated DOEs. Regarding computational time, RDOEs can be calculated efficiently for both networks except when bilinear uncertainty exists in the Australian network. Moreover, setting up the optimisation model for this case can also be computationally demanding. In fact, for the Australian network, it takes at most 9 s to set up the optimisation model when there is a single uncertainty. In comparison, the setup time is as high as 2306.05 s when bilinear uncertainty exists due to a large number of constraints in (31), implying that the computational efficiency can be potentially improved by investigating efficient programming techniques.

V. CONCLUSION

Uncertainties in demand forecasting and impedance modelling in distribution networks are inevitable and could potentially undermine the reliability of calculated DOEs for DER integration. This letter studies the calculation of DOEs when single or bilinear uncertainty exists in demands and network impedances, leading to various tractable formulations. Moreover, uncertainty sets are formulated as generalised norm constraints and could cover the most commonly used measures in quantifying uncertainties. Simulation results show the differences in DOE allocation strategies geometrically with and without considering uncertainties, and demonstrate the efficiency of the proposed approach. Note that the proposed approach is built on a linear UTOPF model, further improving the accuracy in linearising UTOPF and investigating robust formulations under other types of uncertainty sets are potential research directions.

REFERENCES

[1] Distributed Energy Integration Program (DEIP). (2022, Mar.). Dynamic operating envelopes working group outcomes report. [Online]. Available: https://arena. gov. au/assets/2022/03/dynamic-operating-envelope-working-group-outcomes-report.pdf
[2] ENA and AEMO. (2020, Dec.). Open energy networks project – energy networks Australia position paper. [Online]. Available: https://tinyurl.com/4bd9tr5n

[3] K. Petrou, A. T. Procopiou, L. Gutierrez-Lagos *et al.*, "Ensuring distribution network integrity using dynamic operating limits for prosumers," *IEEE Transactions on Smart Grid*, vol. 12, no. 5, pp. 3877-3888, May 2021.

[4] B. Liu and J. H. Braslavsky, "Sensitivity and robustness issues of operating envelopes in unbalanced distribution networks," *IEEE Access*, vol. 10, pp. 92789-92798, Sept. 2022.

[5] W. Wei, F. Liu, and S. Mei, "Real-time dispatchability of bulk power systems with volatile renewable generations," *IEEE Transactions on Sustainable Energy*, vol. 6, no. 3, pp. 738-747, Apr. 2015.

[6] S. Riaz and P. Mancarella, "Modelling and characterisation of flexibility from distributed energy resources," *IEEE Transactions on Power Systems*, vol. 37, no. 1, pp. 38-50, Jan. 2022.

[7] H. Ahmadi, J. R. Marti, and A. von Meier, "A linear power flow formulation for three-phase distribution systems," *IEEE Transactions on Power Systems*, vol. 31, no. 6, pp. 5012-5021, Nov. 2016.

[8] R. A. Horn, R. A. Horn, and C. R. Johnson, *Topics in Matrix Analysis*. Cambridge: Cambridge University Press, 1994.

[9] D. Bertsimas and D. D. Hertog, *Robust and Adaptive Optimization*. Massachusetts: Dynamics Ideas LCC, 2022.

[10] S. Boyd and L. Vandenberghe, *Convex Optimization*. Cambridge: Cambridge University Press, 2004.

[11] B. Liu and J. H. Braslavsky, "Robust dynamic operating envelopes for DER integration in unbalanced distribution networks," *IEEE Transactions on Power Systems*, doi: 10.1109/TPWRS.2023.3308104.

[12] J. Zhong, B. Liu, X. Yu *et al*., "Enhancing voltage compliance in distribution network under cloud and edge computing framework," *IEEE Transactions on Cloud Computing*, vol. 11, no. 2, pp. 1217-1229, 2023.

[13] Mosek. (2023, Jun.). Mosek documentation. [Online]. Available: https://www.mosek.com/documentation

[14] D. M. Fobes, S. Claeys, F. Geth *et al*., "PowerModelsDistribution.jl: an open-source framework for exploring distribution power flow formulations," *Electric Power Systems Research*, vol. 189, p. 106664, Dec. 2020.

Bin Liu received the Bachelor, Master, and Ph.D. degrees from Wuhan University, Wuhan, China, China Electric Power Research Institute, Beijing, China, and Tsinghua University, Beijing, China, in 2009, 2012, and 2015, respectively, all in electrical engineering. He is a Senior Power System Engineer in the Network Planning Division, Transgrid, Sydney, Australia. Before joining Transgrid, he had held research or engineering positions with the Energy Centre, Commonwealth Scientific and Industrial Research Organisation (CSIRO), Newcastle, Australia, The University of New South Wales, Sydney, Australia, State Grid Corporation, Beijing, China, and The Hong Kong Polytechnic University, Hong Kong, China. His current research interests include power system modelling, analysis & planning, optimisation theory applications in the power and energy sector, and the integration of renewable energy including distributed energy resources (DERs).

Julio H. Braslavsky received the Ph. D. degree in electrical engineering from the University of Newcastle, Newcastle, Australia, in 1996, and the Electronics Engineer degree from the National University of Rosario, Rosario, Argentina, in 1989. He is a Principal Research Scientist with the Energy Systems Program of the Australian Commonwealth Scientific and Industrial Research Organisation (CSIRO) and an Adjunct Senior Lecturer with The University of Newcastle, Newcastle, Australia. He has held research appointments with the University of Newcastle, the Argentinian National Research Council, the University of California at Santa Barbara, and the Catholic University of Louvain-la-Neuve in Belgium. He is Senior Editor for IEEE Transactions on Control Systems Technology. His current research interests include modelling and control of flexible electric loads and integration of distributed power-electronics-based energy resources in power systems.

Nariman Mahdavi received the Ph.D. (first class) degree in electrical engineering from the Amirkabir University of Technology, Tehran, Iran, in 2011. He is a Senior Research Scientist with Power Systems and Controls, Energy Centre, Commonwealth Scientific and Industrial Research Organisation (CSIRO), Newcastle, Australia. Prior to joining CSIRO in 2017, he was a Postdoctoral Researcher with The University of Newcastle, Newcastle, Australia, in collaboration with CSIRO Energy Centre, and held research appointments with the Potsdam Institute for Climate Impact Research, Potsdam, Germany. His research interests include mathematical modelling, analysis, estimation and control of dynamical systems to help navigate through the transformation across the energy sector.